

CHE 85-14500). We thank Guy Bemis for helpful discussions.

Registry No. 6a, 65651-52-7; 6b, 72724-02-8; 7 (isomer 1), 131905-98-1; 7 (isomer 2), 89393-62-4; 7 (isomer 3), 131906-33-7; 7 (isomer 4), 131906-34-8; 8a, 89393-74-8; 8b, 108056-65-1; 9, 122088-92-0; 9a, 122020-03-5; 9b, 108056-64-0; 10a, 131905-99-2; 10b, 131906-00-8; 11a, 131906-01-9; 11b, 131906-02-0; 12, 131906-03-1; 12a, 132015-37-3; 12b, 132015-38-4; 13, 131906-04-2; 13a, 132046-17-4; 13b, 132046-18-5; 14a, 122088-88-4; 14b, 122088-89-5; 15a, 122020-04-6; 15b, 122020-05-7; 16, 91094-99-4; 16a, 117020-31-2; 17, 131906-05-3; 17a, 132015-39-5; 18, 17895-71-5;

19, 131906-06-4; 20, 131906-07-5; 21, 131906-08-6; 22, 4160-80-9; 23, 131906-09-7; 24, 131906-10-0; 25, 132015-40-8; 26, 131906-11-1; 27, 131906-12-2; 28, 132015-41-9; 29, 131906-13-3; 30, 131906-14-4; 31, 131906-15-5; 32, 131906-16-6; 33, 131906-17-7; 34, 132015-42-0; 35, 131906-18-8; 36, 131906-19-9; 37, 131906-20-2; 38, 131906-21-3; 39, 131906-22-4; 40, 132015-43-1; 41, 131906-23-5; 42, 131906-24-6; 43, 126575-05-1; 44, 64482-09-3; 45, 131906-25-7; 46, 64482-08-2; 47, 131906-26-8; 48, 131906-27-9; 49, 131906-28-0; 50, 131906-29-1; 51, 131906-30-4; 52, 131906-31-5; 54, 131906-32-6; hydrocinnamic acid, 501-52-0; 3-phenylglutaric acid, 4165-96-2; *tert*-butyl acetate, 540-88-5; 3-amino-3-phenylpropanoic acid, 3646-50-2; α -chymotrypsin, 9004-07-3.

Biologically Active Taxol Analogues with Deleted A-Ring Side Chain Substituents and Variable C-2' Configurations

Charles S. Swindell* and Nancy E. Krauss

Department of Chemistry, Bryn Mawr College, Bryn Mawr, Pennsylvania 19010

Susan B. Horwitz*

Department of Molecular Pharmacology, Albert Einstein College of Medicine, Bronx, New York 10461

Israel Ringel*

Department of Pharmacology, School of Medicine, The Hebrew University, Jerusalem, Israel. Received September 24, 1990

Taxol (1), a potent inhibitor of cell replication, enhances the assembly of tubulin into stable microtubules and promotes the formation of microtubule bundles in cells. In addition to its unique mechanism of action, taxol exhibits unusual promise as an antitumor agent, but its application in cancer chemotherapy is hampered by its limited availability. In order to better define the structure-activity profile of taxol for the design of more accessible drugs and to provide insight into the chemical features of the taxol-microtubule interaction, taxol analogues 3-8, with deleted A-ring side chain substituents and both *R* and *S* C-2' configurations, were synthesized from baccatin III (2) through esterification at the hindered 13-hydroxyl. Employing an improved hydroxyl protection strategy, lactate analogues 3 and 4 were prepared with reasonable efficiency owing to their simple side-chain structures, while *N*-benzoylisoserine analogues 7 and 8 were synthesized through esterification reactions whose rates were enhanced greatly by the participation of the amide functionality. Although less biologically active than taxol, analogues 5-7 were found to promote the polymerization of tubulin and to be cytotoxic; 5 and 6 were considerably more effective than 7, whereas 3, 4, and 8 were least active. Interestingly, tubulin polymerization was sensitive to the C-2' configuration only when the amide substituent was present in the side chain. This observation suggests that the 3'-amide substituent plays an important role in preorganizing the taxol side chain to bind to microtubules.

Introduction

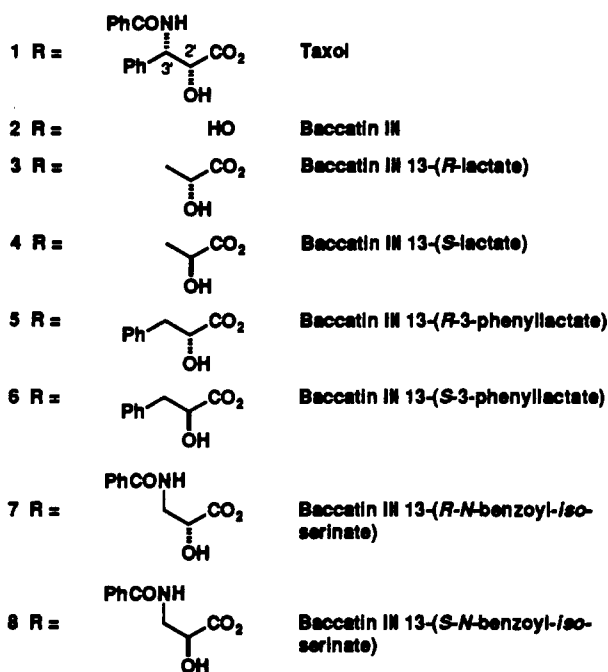
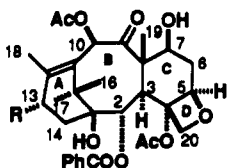
Taxol¹ (1) is unique among antimetabolic drugs in that it promotes the assembly of stable microtubules from tubulin under otherwise unfavorable conditions, i.e. low temperature, the absence of microtubule associated proteins or exogenous GTP, and the presence of Ca ions. The drug binds to microtubules, stabilizing them against depolymerization.^{2,3} A presumed consequence of these effects is the significant antitumor activity exhibited by taxol, most notably, at this time, against drug-refractory

human ovarian tumors.⁴ Currently, the only impediment to the more widespread application of taxol in cancer chemotherapy is its extremely limited availability: taxol is isolated in exceptionally poor yield from the bark of the slow-growing Pacific yew (*Taxus brevifolia*; 1 kg of taxol/20 000 lb of bark from 2000-3000 yew trees),⁵ which is indigenous to the ecologically threatened old-growth forests of the Pacific northwest.

Since the initial biological evaluation of taxol and baccatin III (2) that established the critical role played by the taxol A-ring side chain,¹ the insignificance of the identity of the acyl group on the 3'-amino substituent, and the importance of the 2'-hydroxyl have become apparent.^{3,6} We have sought to define further the taxol structure-activity profile for the locus of the side chain with two

- (1) Wani, M. C.; Taylor, H. L.; Wall, M. E.; Coggon, P.; McPhail, A. T. *J. Am. Chem. Soc.* 1971, 93, 2325.
- (2) Schiff, P. B.; Fant, J.; Horwitz, S. B. *Nature* 1979, 277, 665.
- (3) Schiff, P. B.; Horwitz, S. B. *Proc. Natl. Acad. Sci. U.S.A.* 1980, 77, 1561. Manfredi, J. J.; Horwitz, S. B. *Pharmacol. Ther.* 1984, 25, 83.
- (4) Horwitz, S. B.; Lothstein, L.; Manfredi, J. J.; Mellado, W.; Parness, J.; Roy, S. N.; Schiff, P. B.; Sorbara, L.; Zeheb, R. *Ann. N.Y. Acad. Sci.* 1986, 466, 733. Horwitz, S. B.; Schiff, P. B.; Parness, J.; Manfredi, J. J.; Mellado, W.; Roy, S. N. In *The Cytoskeleton*; Clarkson, T. W., Sager, P. R., Syversen, T. L., Eds.; Plenum: New York, 1986.

- (4) McGuire, W. P.; Rowinsky, E. K.; Rosenchein, N. B.; Grumbine, F. C.; Ettinger, D. S.; Armstrong, D. K.; Donehower, R. C. *Ann. Intern. Med.* 1989, 111, 273.
- (5) Rowinsky, E. K.; Casenave, L. A.; Donehower, R. C. *J. Natl. Cancer Inst.* 1990, 82, 1247.
- (6) Kingston, D. G. I.; Samaranyake, G.; Ivey, C. A. *J. Nat. Prod.* 1990, 53, 1.

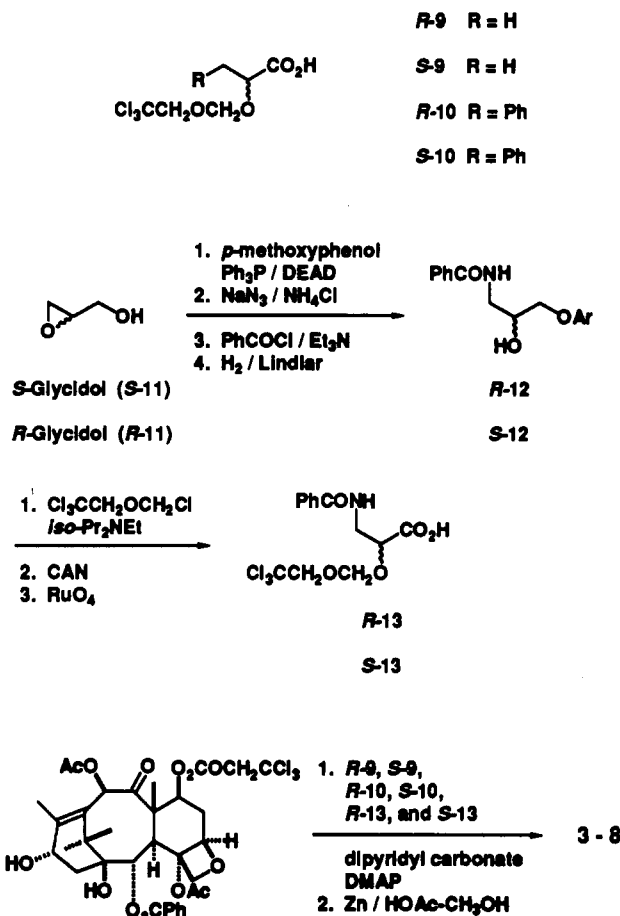


principal aims in mind. First, one approach to improving the availability of substances medicinally similar to taxol is through the identification of active analogues that might be readily synthesized from abundant but inactive taxanes. For example, 10-deacetylbaccatin III (cf. 2) is reported to be available in good yield from the (renewable) leaves of the ornamental yew *T. baccata* (1 g of 10-deacetylbaccatin III/1 kg of leaves), and has been converted through a tedious esterification to taxol.⁷ Analogues that bear structurally simpler side chains might be partially synthesized more effectively, but their identification requires a more extensive knowledge of the structure-activity parameters for taxol. Second, knowledge of this kind will aid in defining some of the features of the taxol binding site on microtubules. Herein, we report the syntheses and biological evaluation of deletion analogues 3-8. In addition to expanding the taxol structure-activity database, this work has led to some insight into the side chain attachment chemistry, and has provided the first glimpse into the detailed structural and stereochemical requirements for the recognition of taxol and some analogues by microtubules.

Chemistry

The syntheses of taxol analogues 3-8 were carried out by coupling the appropriate carboxylic acids bearing protected 2'-hydroxyls to the highly hindered 13-hydroxyl of 7-hydroxyl-protected baccatin III. One of the pitfalls of the taxol partial synthesis devised by Greene and Guéritte-Voegelein⁷ was the instability during the lengthy esterification of the acid-labile 2'-ethoxyethyl ether protected side chain carboxylic acid. The protection strategy employed in the preparation of 3-8 avoids this difficulty by pairing acid-stable (trichloroethoxy)methyl ether pro-

Scheme I



tected⁸ side chain acids with baccatin III 7-trichloroethyl carbonate⁹ (14; Scheme I). Concomitant deprotection of both the 7- and 2'-hydroxyls is then achievable in one experimental operation through the treatment of the coupling products with Zn.^{8,9}

Thus according to this plan, the six optically active acids 9, 10, and 13 were required (Scheme I). Protected hydroxy acids 9 and 10 were obtained readily from the corresponding *R* and *S* methyl lactates and methyl phenyllactates¹⁰ through their sequential reaction with (trichloroethoxy)methyl chloride and saponification. As expected, these substances were conveniently stable. Iso-serine derivatives 13 were prepared from the commercially available glycidol enantiomers 11. The protection of the primary hydroxyl in 11 through the formation of the *p*-methoxyphenyl ether¹¹ was followed by regioselective epoxide opening with azide ion,¹² O-benzoylation, and azide reduction¹³ with ensuing benzoyl migration. Hydroxy amides 12 were then protected, as above, at the 2'-hydroxyl, and the primary alcohol deprotected with ceric

(7) Greene, A. E.; Denis, J.-N.; Guénard, D.; Guéritte-Voegelein, F.; Mangatal, L.; Potier, P. *J. Am. Chem. Soc.* 1988, 110, 5917.

(8) Salomaa, D.; Linnantie, R. *Acta Chem. Scand.* 1960, 14, 777.

Jacobson, R. M.; Clader, J. W. *Synth. Commun.* 1979, 9, 57.

(9) Magri, N. F.; Kingston, D. G. I.; Jitrangri, C.; Piccarriello, T. *J. Org. Chem.* 1986, 51, 3239.

(10) Marsman, B.; Wynberg, H. *J. Org. Chem.* 1979, 44, 2312. Mor, G.; Ehret, A.; Cohen, S. G. *Arch. Biochem. Biophys.* 1976, 174, 158.

(11) Fukuyama, T.; Laird, A. A.; Hotchkiss, L. M. *Tetrahedron Lett.* 1985, 26, 6291.

(12) Behrens, C. H.; Sharpless, K. B. *Aldrichimica Acta* 1983, 16, 67.

(13) Corey, E. J.; Nicolaou, K. C.; Balanson, R. D.; Machida, Y. *Synthesis* 1975, 590.

Table I. 300-MHz ^1H NMR Data for 3-8 Recorded in CDCl_3^a

protons on:	3	4	5	6	7	8
C-2	5.68 (d, 7)	5.67 (d, 7)	5.65 (d, 7)	5.67 (d, 7)	5.67 (d, 7)	5.67 (d, 7)
C-3	3.83 (d, 7)	3.83 (d, 7)	3.76 (d, 7)	3.82 (d, 7)	3.81 (d, 6.3)	3.86 (d, 6.4)
C-5	4.98 (d, 7.7)	4.97 (d, 7.7)	4.94 (d, 7.6)	4.97 (d, 7.8)	4.96 (d, 7.8)	4.98 (d, 8.1)
C-6	1.8-1.9, 2.5-2.6 (m)	1.8-1.9, 2.5-2.6 (m)	1.8-1.9, 2.5-2.6 (m)	1.8-1.9, 2.5-2.6 (m)	1.8-1.9, 2.5-2.6 (m)	1.8-1.9, 2.5-2.6 (m)
C-7	4.4-4.5 (m)	4.43 (dd, 6, 9)	4.40 (dd, 6.8, 10.6)	4.42 (dd, 6.6, 10.8)	4.4-4.5 (m)	4.4-4.5 (m)
C-10	6.31 (s)	6.30 (s)	6.46 (s)	6.30 (s)	6.29 (s)	6.32 (s)
C-13	6.26 (t, 9)	6.29 (t, 9.5)	6.17 (t, 9)	6.24 (t, 8.9)	6.24 (t, 8.7)	6.23 (t, 8.3)
C-14	2.2-2.3 (m)	2.2-2.3 (m)	2.14 (d, 9)	2.2-2.3 (m)	2.2-2.3 (m)	2.2-2.3 (m)
C-16	1.27 (s)	1.25 (s)	1.25 (s)	1.26 (s)	1.24 (s)	1.25 (s)
C-17	1.16 (s)	1.16 (s)	1.14 (s)	1.16 (s)	1.15 (s)	1.15 (s)
C-18	1.92 (s)	1.92 (s)	1.76 (s)	1.86 (s)	1.87 (s)	2.02 (s)
C-19	1.69 (s)	1.69 (s)	1.67 (s)	1.69 (s)	1.68 (s)	1.68 (s)
C-20	4.17, 4.33 (AB q, 8.4)	4.17, 4.31 (AB q, 8.3)	4.15, 4.29 (AB q, 8.4)	4.17, 4.31 (AB q, 8.4)	4.18, 4.31 (AB q, 8.3)	4.16, 4.31 (AB q, 8.4)
OAc	2.26, 2.35 (s)	2.26, 2.31 (s)	2.23, 2.25 (s)	2.26, 2.29 (s)	2.23, 2.44 (s)	2.24, 2.40 (s)
PhCO	7.50 (t, 7.4), 7.64 (t, 7.4), 8.09 (dd, 1.5, 7.1)	7.49 (t, 7.4), 7.63 (t, 7.3), 8.07 (dd, 1.5, 8.5)	7.52 (t, 7.4), 7.65 (t, 6.2), 8.08 (dd, 1.4, 8.5)	7.50 (t, 7.4), 7.63 (t, 6.1), 8.06 (dd, 1.4, 8.4)	7.4-7.5 (m), 7.62 (t, 7.4), 7.76 (dd, 1.5, 8.6), 8.10 (dd, 1.5, 8.6)	7.4-7.6 (m), 7.62 (t, 7.4), 7.77 (dd, 1.5, 8.6), 8.07 (dd, 1.5, 8.6)
C-2'	4.42 (q, 6.9)	4.37 (q, 6.9)	4.53 (t, 5.7)	4.51 (dd, 4.4, 8)	4.4-4.5 (m)	4.4-4.5 (m)
C-3'	1.51 (d, 6.9)	1.59 (d, 6.9)	3.13 (d AB q, 5.7, 12.9)	3.04 ($^1/2$ d AB q, 8, 14), 3.29 ($^1/2$ d AB q, 4.4, 14)	3.8-3.9 (m)	3.8-3.9 (m), 4.06 ($^1/2$ dd AB q, 3.7, 5.7, 14)
Ph			7.2-7.4 (m)	7.2-7.4 (m)		
NH					6.78 (t, 5.7)	6.63 (t, 5.7)

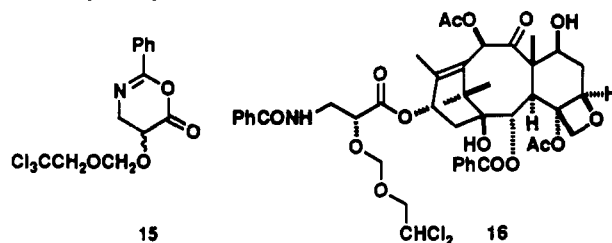
^a Multiplicities are indicated in parentheses with coupling constants in hertz. Apparent multiplicities are described in many instances.

ammonium nitrate (CAN)¹¹ and oxidized¹⁴ to deliver 2'-hydroxyl-masked *N*-benzoylisoserines 13. Again, these intermediates were satisfactorily stable. Note that a change upon epoxide cleavage of the 2'-substituent Cahn-Ingold-Prelog priorities requires that the (*R*)-isoserine derivative be synthesized from (*S*)-glycidol, and vice versa.

The syntheses of baccatin III 13-lactate and 13-(3-phenyllactate) derivatives 3-6 were carried out by the esterification of 9 and 10 with 14 mediated by dipyridyl carbonate¹⁵ according to the Greene and Guéritte-Voegelein protocol.⁷ Deprotection of the coupling products provided, after chromatographic purification, 3-6. In this series, there was a clear dependence of the efficiency of the esterification-deprotection procedure on side-chain complexity: 3 and 4 were each obtained in about 50% overall yield while 5 and 6 were each isolated in approximately 30% overall yield. These yields were dictated by the esterification steps as the deprotections were essentially quantitative. Significantly, epimerization at the 2'-position occurred to a minor degree in these coupling-deprotection processes; the epimeric impurities were removed by HPLC prior to biological evaluation, in each case.

In contrast to the experience with 3-6, 7, and 8 were produced through esterifications that proceeded with unanticipated high rates. Under the conditions described in the Experimental Section, the esterifications that led to 3-6 required 48 h for completion, while those involved in the production of 7 and 8 consumed 14 in approximately 6 h. Considering the functional differences between the 9/10 series and 13, it seems likely that 5,6-dihydro-6-ketooxazine intermediates 15 intervened in esterifications of the latter. 5,6-Dihydro-6-ketooxazines, cyclic versions of the activated esters that mediate carbodiimide-induced acylations, have been formed from amido acids similar to 13, and have been shown to be acylation agents.¹⁶ 5,6-Dihydro-6-ketooxazines 15 would be less sterically demanding and consequently more reactive toward the baccatin III 13-hydroxyl than electrophilic intermediates

formed from less functionalized acids 9 and 10. An intermediate of this kind might have participated in the taxol partial synthesis of Greene and Guéritte-Voegelein,⁷ with its rate of formation or reactivity compromised by the 3'-phenyl substituent missing in 13. In any case, 5,6-dihydro-6-ketooxazine acylating agents prepared through more efficient independent or in situ chemistry might provide a generally effective way of acylating the baccatin III 13-hydroxyl.¹⁷



From the coupling-deprotection sequence beginning with *R*-13 and 14, taxol analogue 7 was isolated in 46% yield along with 39% of byproduct 16. Although prolonged treatment of 16 with Zn failed to convert it to 7, its detection indicates that the coupling process proceeded with at least 85% efficiency. Inexplicably, the sequence beginning with *S*-13 and 14 was not similarly complicated and provided 8 in 94% yield. Furthermore, materials analogous to 16 did not appear to complicate the syntheses of 3-6, so they do not pose a general limitation to the hydroxyl protection scheme employed in this work. The production of C-2' epimeric impurities was more serious in the preparations of 7 (89% epimerically pure; 78% de) and 8 (85% epimerically pure; 70% de). Since Mosher ester analyses¹⁸ carried out on 11 indicated their optical purities to each be 90% ee, epimerization must have oc-

(14) Sharpless, K. B.; Carlsen, P. H. J.; Katsuki, T.; Martin, V. S. *J. Org. Chem.* 1981, 46, 3936.

(15) Kim, S.; Lee, J. I.; Ko, Y. K. *Tetrahedron Lett.* 1984, 25, 4943.

(16) Barker, C. C. *J. Chem. Soc.* 1954, 317.

(17) Preliminary experiments involving *R*-13 and *S*-13 have shown their thionyl chloride treatment to deliver materials whose ^{13}C NMR parameters (single carbonyl at 172.7 ppm; imidate quaternary at 146.5 ppm) are consistent with 15. Furthermore, the treatment of *R*-13 and *S*-13 with trifluoromethanesulfonic anhydride (triflic anhydride)/2,6-di-*tert*-butylpyridine provides intermediates that upon exposure to 14 give the protected forms of 7 and 8, respectively.

(18) Dale, J. A.; Dull, D. L.; Mosher, H. S. *J. Org. Chem.* 1969, 34, 2543.

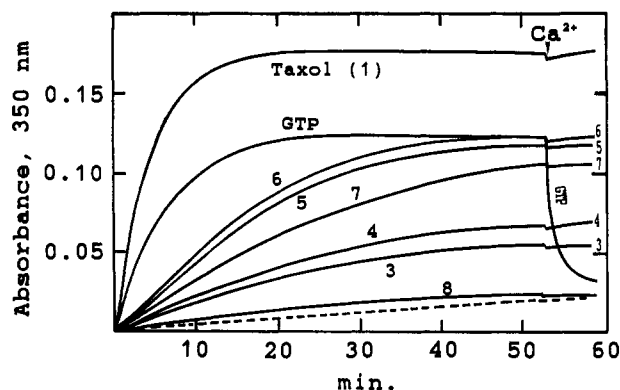


Figure 1. Assembly of MTP in the presence of GTP, taxol, or 3–8. MTP (1.5 mg/mL) was incubated at 35 °C with 15 μ M taxol or 3–8 (added as DMSO solutions; 1% final DMSO concentration) in the absence of GTP. The assembly reactions were followed by turbidity measurements at 350 nm. At the time denoted, 4 mM CaCl_2 was added to each experimental sample. Slow aggregation and assembly in the presence of 1% DMSO alone shown by dashed curve.

Table II. The Extents and Initial Rates of MTP Assembly in the Presence of Taxol, GTP, or 3–7^a

drug	% assembly	initial slope (AU/min $\times 10^{-2}$)	rel initial slope
taxol	100	3.57	100
GTP	70	2.42	67.7
3	31	0.20	5.6
4	38	0.23	6.4
5	68	0.47	13.2
6	69	0.56	15.7
7	60	0.20	5.6

^a 1.5 mg/mL MTP + 15 μ M drug (1% DMSO).

currred at the stage of 13 or during the coupling–deprotection sequences. As in the case of 3–6, epimeric impurities associated with 7 and 8 were resolved and eliminated through HPLC.

The structures of 3–8 were verified readily from their spectral characteristics. Molecular formulas were confirmed by high-resolution fast atom bombardment (FAB) mass measurements of (M + Na) or (M + H) ions. The ^1H NMR spectra exhibited by 3–8 are consistent with data available for related taxane diterpenes and their derivatives¹⁹ (Table I). In particular, it was clear from each of these spectra that the baccatin III nucleus had been esterified at the C-13 hydroxyl, and that the appropriate new elements of the side chain had been incorporated. Furthermore, the configurational differences at C-2' in the epimeric pairs of lactates, 3-phenyllactates, and *N*-benzoylisoserinates, respectively, are reflected in their ^1H NMR spectra. For the lactates (3 and 4), the chemical shift of the C-3' methyl doublet resonance is most diagnostic of C-2' configuration. Similarly, the 3-phenyllactates (5 and 6) and the *N*-benzoylisoserinates (7 and 8) exhibit pronounced differences in the spectral behavior of the diastereotopic C-3' methylene protons: in the *R* derivatives, these resonances are very nearly coincident while the corresponding signals of the *S* diastereomers are quite disparate.

Biological Results

Effect of Taxol and Analogues on Microtubule Assembly. Microtubule assembly *in vitro* normally requires GTP. However, the hallmark of taxol is its ability to assemble stable microtubules in the absence of GTP.

Table III. Drug Sensitivity of J774.2 and CHO Cells

drug	ED ₅₀ , ^a μ M	
	J774.2	CHO
taxol	0.09	0.35
3	27.00	>45.00
4	29.00	>45.00
5	3.50	5.50
6	3.40	5.30
7	20.00	32.00

^a ED₅₀: drug concentration that inhibits cell division by 50% after 72 h.

Therefore, the effect of analogues 3–8 on microtubule assembly in the absence of GTP was studied (Figure 1). Microtubule protein (MTP; 1.5 mg/mL) was incubated at 35 °C with 15 μ M drug. Table II summarizes the parameters of MTP assembly in the presence of 3–7, and compares them to those obtained with GTP and taxol; the extent of MTP assembly in the presence of 8 is negligible, with the observed turbidity due to aggregates formed in the presence of DMSO in this case. The steady-state level of microtubules formed in the presence of 5 and 6 is comparable to that achieved in the presence of GTP while 7 is somewhat less effective in promoting microtubule assembly. Baccatin III (2) is inactive in this assay.²⁰ All of the initial slope values obtained in the presence of the analogues are reduced compared to those observed with GTP. These findings suggest that 3–7 are less potent than taxol or GTP in enhancing the nucleation phase of assembly. However, all of the polymers assembled in the presence of the taxol analogues were stable toward calcium ion induced depolymerization, while those assembled in the presence of GTP were not. The slower rate of assembly in the presence of 3–7 compared to taxol contributes to the orderly organization of microtubules. No hoops or ribbons, which are part of the polymeric mass assembled in the presence of taxol,²¹ could be detected by electron microscopy (data not shown).

Effect of Taxol and Analogues on Cell Replication and Microtubule Bundle Formation. The ED₅₀ (drug concentration that inhibits cell division by 50% after 72 h) for J774.2 and CHO cells by 3–8 was determined with a range of drug concentrations. From Table III, it can be observed that 5 and 6 are approximately 15–40-fold less cytotoxic than taxol, depending on the cell line, whereas 3, 4, and 7 exhibit significantly less activity. Although no significant difference in potency could be discerned for *R* and *S* diastereomers 3 and 4, or 5 and 6, in J774.2 cells, *S* isomer 8 did not achieve 50% growth inhibition even at the highest concentration (45 μ M) of drug used, whereas *R* isomer 7 achieved 50% growth inhibition at 20 μ M of drug. This parallels the behavior of these six analogues in the tubulin assembly studies.

The incubation of cells in the presence of taxol results in the formation of bundles of highly ordered arrays of microtubules.²² To determine the effect of 5–7 on cellular microtubules, CHO cells were grown on coverslips for 24 h at which time the medium was replaced with fresh medium containing several concentrations of drugs. The effects of the drugs on the microtubule cytoskeleton was examined by immunofluorescence microscopy using tu-

(19) See, for example: Miller, R. W. *J. Natl. Prod.* 1980, 43, 425.

(20) Parness, J.; Kingston, D. G. I.; Powell, R. G.; Harracksingh, C.; Horwitz, S. B. *Biochem. Biophys. Res. Commun.* 1982, 105, 1082.

(21) Parness, J.; Horwitz, S. B. *J. Cell Biol.* 1981, 91, 479.

(22) Schiff, P. B.; Horwitz, S. B. *Proc. Natl. Acad. Sci. U.S.A.* 1980, 77, 1561. DeBrabander, M.; Gevens, G.; Nuydens, R.; Willebrords, R.; Demay, J. *Proc. Natl. Acad. Sci. U.S.A.* 1981, 78, 5608.

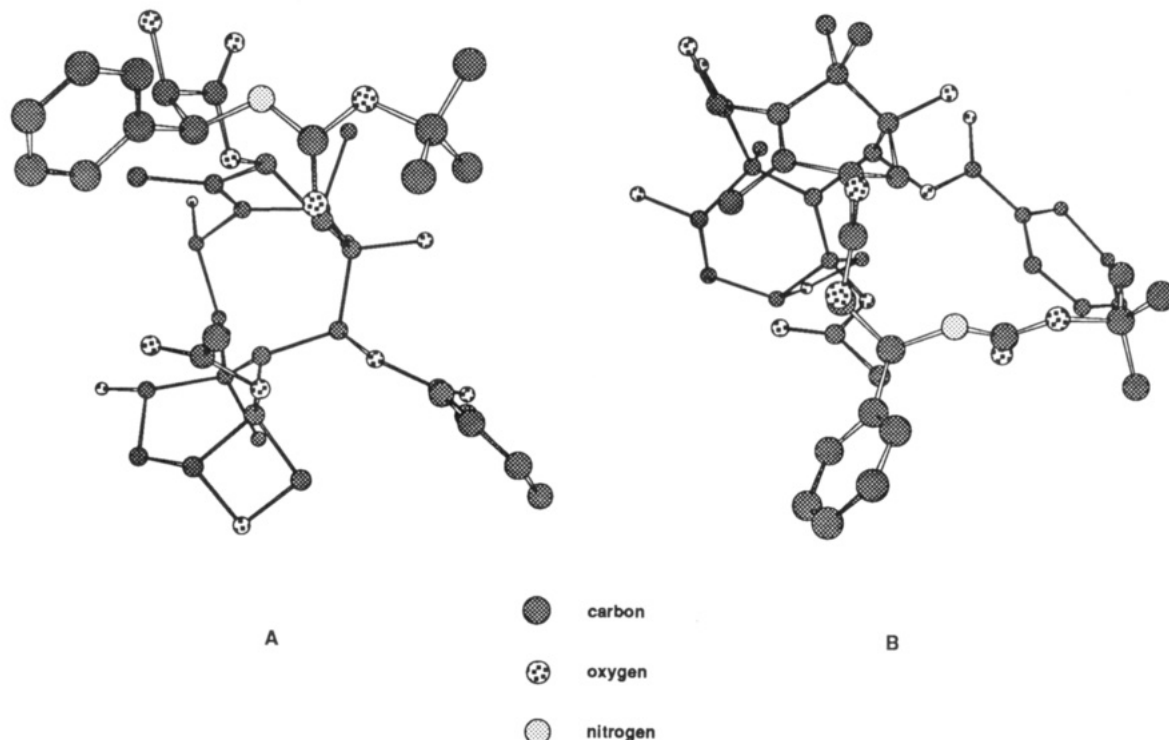


Figure 2. Crystal structure of taxotere (17) viewed with the A-ring side chain in the foreground. Orientation B is viewed along the side chain carboxyl carbon-oxygen single bond with the oxygen-C-13 bond in a vertical plane perpendicular to the page. Hydrogen atoms are deleted. Fractional coordinates are taken from ref 23.

Table IV. Solubility of Taxol and 3-8^a

drug	H ₂ O, μ M	CHCl ₃ /H ₂ O	octanol/H ₂ O
taxol	35	>1000	>1000
3	820	160	33
4	1000	170	35
5	175	340	800
6	160	320	800
7	615	200	56
8	565	230	84

^aAll measurements were performed by reverse-phase HPLC (Merck-Hitachi instrument; methanol-water, 65:35).

bulin antibodies. At the ED₅₀ concentrations of both taxol and 5-7, there was no significant difference between the ability of taxol and the analogues to induce the formation of microtubule bundles in CHO cells (data not shown).

Water Solubility of Taxol and Analogues. One of the major drawbacks of taxol as a prospective antitumor drug is its low water solubility that complicates its formulation. We examined the water solubility of analogues 3-8 by three different methods. In the first, an excess of drug was mixed vigorously with and sonicated in distilled water. The suspension was centrifuged and the clear supernatant analyzed for drug concentration. In the second and third, each compound was distributed between a two-phase mixture of chloroform-water and octanol-water, respectively. The samples were mixed vigorously for 1 h, and after separation of the two phases, each phase was examined by HPLC. The evaluation of drug concentration by HPLC is superior to determination by measurement of UV absorbance as it eliminates interference by products of drug degradation (i.e. hydrolysis). Table IV summarizes the results. All of the analogues have better water solubility than does taxol. Within the set of analogues investigated, hydrophilicity ranges, as might be expected, from the most soluble lactates (3 and 4) that lack a 3'-substituent, through the moderately soluble *N*-benzoyl-isoserinates (7 and 8) that have a modestly polar benzamido group at C-3', to the least soluble phenyllactates (5

and 6) with the hydrophobic phenyl positioned at the termini of their side chains.

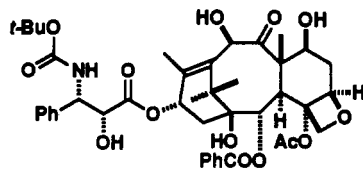
Discussion

Although there is a range of tubulin polymerization activities associated with taxol analogues 3-8, it is encouraging from the point of view of analogue design that the rather profound structural alterations encompassed by this group still support reasonable activity. Nevertheless, it is obvious that certain features of the taxol side chain enhance activity. In particular, the presence of a hydrophobic residue at the terminus, as in phenyllactates 5 and 6, is apparently advantageous. This is somewhat unfortunate given the need for a taxol analogue with better formulation properties⁵ and the poor aqueous solubility associated with the presence of the taxol side chain. According to our measurements, the maximum water solubility of baccatin III is 1.44 mM, which is ca. 40 times higher than the solubility of taxol (see Table IV).

The most impressive aspect of the structure-activity function for 3-8, however, is related to the side chain C-2' configuration. Surprisingly, there is little dependence of activity on stereochemistry at that site in the lactate and phenyllactate analogues. Indeed, the unnatural *S* configuration in each diastereomeric pair appears to support slightly better activity. In contrast, when the amide substituent is retained in the side chain, significant dependence on C-2' configuration is turned on such that the natural *R* configuration is preferred. Cast in terms of affinities for the binding site on microtubules, the two phenyllactate analogues would be equally avid ligands while the two *N*-benzoyl-isoserine analogues would not. Although the presence of the 3'-amide substituent is not obligatory for activity, as the results with 5 and 6 attest, it seems likely that when it does form a part of the side chain, the way in which it organizes that structure is important.

To gain some insight into this point, it is useful to consider the recently reported crystal structure of the taxol

analogue taxotere²³ (17; Figure 2), the first crystal structure available for a biologically active taxane possessing an A-ring side chain. Taxotere is as effective as taxol at



17 Taxotere

promoting the assembly of microtubules and approximately twice as cytotoxic.²⁴ The solid-state structure of taxotere shows that in its side chain, there is sequential hydrogen bonding between the ester carbonyl, the 2'-hydroxyl, and the 3'-NH. Together with the C-2' and C-3' configurations, these interactions impose a well-defined conformation on the side chain. It is not unreasonable that these conformational details allow taxotere to be preorganized for good binding²⁵ to microtubules. In view of the close similarity between taxotere and taxol, it is likely that their activities are traceable to the same characteristics, and that they arrange their side chains in much the same way.

To test whether the phenyllactate and *N*-benzoylserine side chains mimic conformationally the taxotere side chain, modelling of the corresponding methyl ester conformations was carried out with MM2.²⁶ Two conformational minima were found for each side chain type. Figure 3 depicts the taxotere side chain excised from the taxotere crystal structure and oriented in the two ways (A and B) shown in Figure 2, as well as the two optimized methyl phenyllactate (19 and 20) and the two optimized methyl *N*-benzoylserinate (21 and 22) conformations. Since modelling the methyl esters removes all but the side chain stereogenic centers, the *R* and *S* models are enantiomeric (and therefore isoenergetic), but each structure is displayed in Figure 3 as it would be if connected to the taxane nucleus in the A and B orientations defined in Figure 2. Thus side-chain arrangement in the space near the taxane A ring as a function of C-2' configuration is illustrated. The modelling calculations make it clear that the hydrogen bonding or electrostatic interactions involving the proximate C=O, OH, and NH moieties in the side chains are the major determinants of side chain conformation. It is unlikely that the taxane nucleus influences to a great degree the local conformations of the side chains. The similarity of the ¹H NMR coupling constants involving the 2'-H and the 3'-H in both taxol and the taxol side chain methyl ester ($J_{2,3} = 3$ Hz in taxol;²⁷ $J_{2,3} = 2$ Hz in the side chain methyl ester²⁸), the fact that in taxotere the side chain carboxyl adopts the conventional *Z* conformation,²⁹

Table V. Data for Models 18–22

structure	N3'-C3'-C2'-O2', ^a		rel energy, ^b kcal/mol
	deg		
18	-65	-2	
<i>R</i> -19		+21	0.25
<i>S</i> -19		-21	0.25
<i>R</i> -20		-12	0.0
<i>S</i> -20		+12	0.0
<i>R</i> -21	+48	-13	0.40
<i>S</i> -21	-48	+13	0.40
<i>R</i> -22	-58	-12	0.0
<i>S</i> -22	+58	+12	0.0

^a Significant dihedral angles. Dihedral angles in enantiomeric pairs are related by a factor of -1. ^b Relative energies are comparable only within isomeric groups, i.e. 19/20 and 21/22. Enantiomeric pairs are necessarily isoenergetic.

and the agreement between the taxotere side chain conformation and the relevant portion of the lowest energy conformation calculated for the (*R*)-*N*-benzoylserine methyl ester (*R*-22) bear this out. Important numerical data for the models are given in Table V.

Models 19 and 20 show the possible conformations of the phenyllactate analogues. If these represent the relevant bound conformations, the common theme among them is that they project their hydrophobic phenyl groups in roughly the same way as does the taxotere side chain. On this basis, it can be argued that the C-2' configuration in 5 and 6 plays a minor role in locating the phenyl group and therefore influences to an insignificant degree analogue binding to microtubules. On the other hand, (*R*)-*N*-benzoylserine conformation *R*-22 resembles very closely the taxotere side-chain structure in the way it projects the amide group, but both conformations of the corresponding *S* analogue (*S*-21 and *S*-22) orient the amide function quite differently. In particular, conformation *S*-22 places the benzamide in a region of space unoccupied in any of the other side chain conformers. Whether in (*S*)-*N*-benzoylserine analogue 8 the amide might be oriented so as to interfere with microtubule residues at the binding site (as in *S*-22) or the microtubule binding site is designed to interact with the amide group through specific hydrogen bonding or electrostatic interactions that are disallowed by the side-chain conformation of 8 (either *S*-21 or *S*-22) cannot be said in the absence of direct information on the binding site. If the latter, the interactions are nonobligatory given the activities of the phenyllactate analogues. Furthermore, it is not clear why the side chain of 8 through conformation *S*-21 would not mimic those of 5 and 6 (side chain conformations 19 and 20), which appear to be similar. Perhaps polar forces at the ligation site mitigate against the binding of conformation *S*-21 due to the incorporation of the polar amide function. *In general, the above modelling results combined with the observed taxol analogue activities suggest that the taxol recognition site on microtubules possesses a hydrophobic cleft designed to accept a side chain with the array of functionality preorganized by stereochemistry and hydrogen bonding that is exemplified in taxotere side chain 18.* An appropriately arranged subset of this structure is accepted, as in the case of 5 and 6 (conformations 19 and 20), but an inappropriately arranged subset is not, as in the case of 8 (conformations 21 or 22). According to this analysis, one would expect the C-3' configuration in the more complicated taxol and taxotere side chains to play a critical role as well.

- (23) Guéritte-Voegelein, F.; Guénard, D.; Mangatal, L.; Potier, P.; Guilhem, J.; Cesario, M.; Pascard, C. *Acta Crystallogr.* 1990, C46, 781.
- (24) Ringel, I.; Horwitz, S. B. *J. Natl. Cancer Inst.*, in press.
- (25) Cram, D. J.; Trueblood, K. N. In *Host Guest Complex Chemistry*; Vogtle, E., Weber, E., Eds.; Springer-Verlag: Berlin, 1985; p 1. Cram, D. *J. Angew. Chem., Int. Ed. Engl.* 1986, 25, 1039. Cram, D. *J. Science* 1988, 240, 760.
- (26) Allinger, N. L. *J. Am. Chem. Soc.* 1977, 99, 8127. Sprague, J. T.; Tai, J. C.; Yuh, Y.; Allinger, N. L. *J. Comput. Chem.* 1987, 8, 581. Liljefors, T.; Tai, J. C.; Li, S.; Allinger, N. L. *J. Comput. Chem.* 1987, 8, 1051.
- (27) Kingston, D. G. I.; Hawkins, D. R.; Ovington, L. *J. Nat. Prod.* 1982, 45, 466.
- (28) Denis, J.-N.; Greene, A. E.; Serra, A. A.; Luche, M.-J. *J. Org. Chem.* 1986, 51, 46.

- (29) Williams, G.; Owen, N. L.; Sheridan, J. *Trans. Faraday Soc.* 1971, 67, 922. Wiberg, K. B.; Laidig, K. E. *J. Am. Chem. Soc.* 1987, 109, 5935.

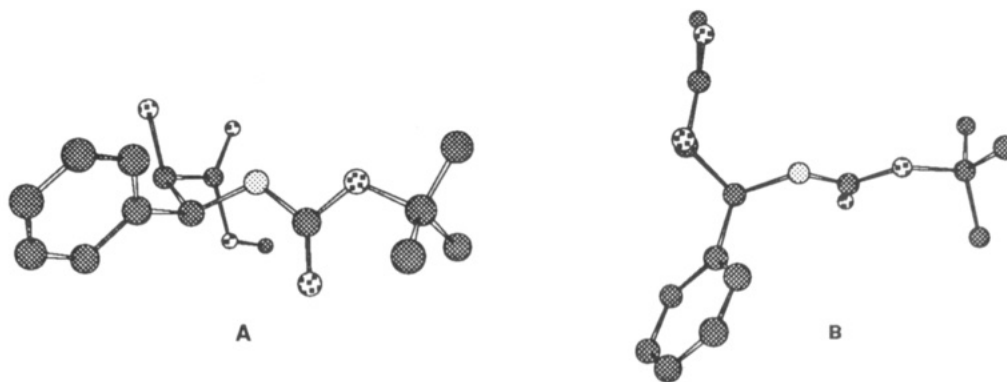
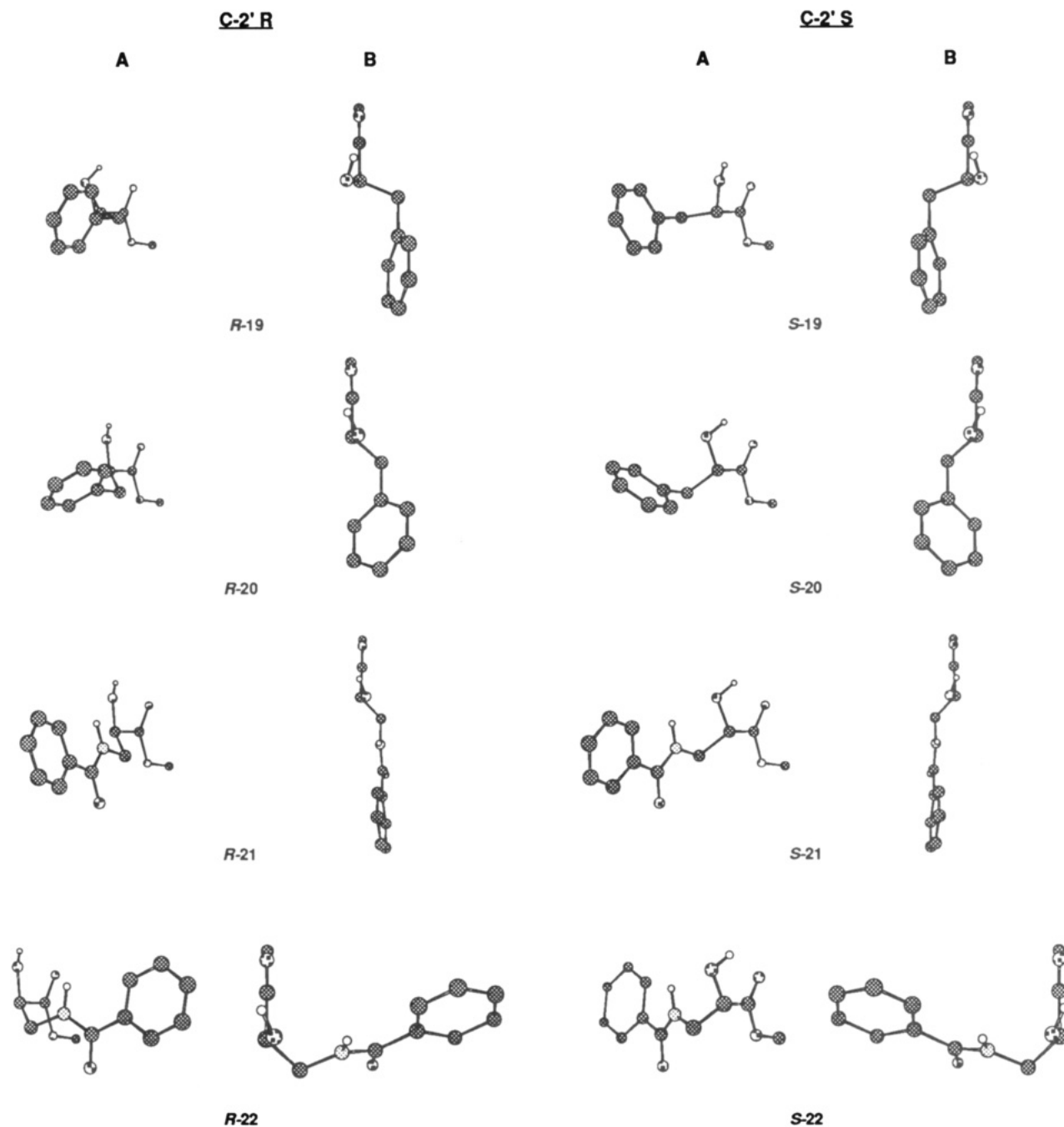
**18 Taxotere Side Chain Plus C-13**

Figure 3. The taxotere side chain excised from the crystal structure and viewed as in A and B, Figure 2, and the optimized conformations of the side-chain methyl esters viewed similarly. Models 19 and 20 are of the methyl phenyllactates and models 21 and 22 are of the methyl *N*-benzoylisoserinates. Most hydrogen atoms are deleted for clarity.

The foregoing is but a very preliminary analysis of some of the structural factors crucial for taxol binding to microtubules. However, testable models of the taxol-microtubule interaction have not been available heretofore to guide work in the area. The ideas presented in this discussion should be subject to verification through more extensive structure-activity studies, the determination of analogue conformations by more thorough modelling, NMR, and crystallographic investigations, and characterization of the binding site on microtubules for taxol, for example, by photoaffinity labeling experiments.

Conclusions

Taxol analogues 3-8 have been prepared from baccatin III. An improved hydroxyl protection protocol enhanced the stability of the precursor side chain acids during their esterification to the baccatin III 13-hydroxyl. The rates of acylation with amido acids 13 were greatly accelerated, probably because of the intervention of 5,6-dihydro-6-ketooxazines 15. This observation suggests a general solution to the problem of acylating efficiently the hindered 13-hydroxyl of baccatin III in the partial synthesis of taxol and analogues. Among 3-8, 5-7 were most effective at promoting the assembly of microtubules from tubulin. Side-chain configuration at C-2' failed to influence activity in the lactate and phenyllactate series, but the natural *R* configuration led to substantially better activity when the 3'-amide group was present in the side chain. These results suggest that the combination of polar interactions and stereochemistry preorganizes the side chain of taxol and its biologically active analogues for effective binding to microtubules.

Experimental Section

Baccatin III³⁰ was prepared as described by Kingston⁹ by degradation of a taxol/cephalomanine mixture provided by Polysciences, Inc., Warrington, PA. Baccatin III 7-trichloroethyl carbonate⁹ (14) and dipyrilidyl carbonate¹⁵ were prepared according to literature procedures. Taxol was obtained from the National Cancer Institute. All drugs were dissolved in DMSO for the biological experiments. The maximum final concentration of DMSO in experimental samples *in vitro* was 1% and in cell culture 0.1%.

¹H NMR spectra (300 MHz) of CDCl₃ solutions were recorded on an IBM NR/AF-300 spectrometer using tetramethylsilane ($\delta = 0$ ppm) or residual chloroform ($\delta = 7.27$ ppm) as the internal standard. ¹³C NMR spectra (75 MHz) of CDCl₃ solutions were determined on the same spectrometer with solvent acting as the internal standard ($\delta = 77$ ppm); degrees of proton substitution were assigned with the aid of 1D DEPT experiments. Ultraviolet spectra of methanol solutions were recorded on a Hewlett-Packard 8452A UV/vis spectrophotometer. HPLC chromatography was carried out with a Waters instrument on a 3.9 mm \times 15 cm Nova-Pak C₁₈ column, or on a 7.8 \times 30 cm Nova-Pak C₁₈ column employing UV detection at 254 nm, or with a Merck-Hitachi instrument on a Lichrosorb C₁₈ column employing UV detection at 230 nm. High-resolution FAB mass spectral determinations were performed at the Mass Spectrometry Laboratory, Department of Chemistry, University of Pennsylvania, Philadelphia, PA. Electron microscopy was carried out on a JEOL 100CX electron microscope at 80 kV.

As only small amounts of HPLC-purified taxol analogues were produced, considerable care was exercised in the determination of the UV extinction coefficients that were used subsequently in quantitating drug solutions for the biological experiments. Weights of samples for UV spectroscopy were determined by the integration of their ¹H NMR spectra in the presence of methanol as integration standard. These solutions (in CDCl₃ solvent) were then diluted in methanol and their UV spectra recorded against

a solvent blank containing an identical methanol-CDCl₃ mixture. The uncertainty in the extinction coefficients is estimated to be $\pm 0.1 \times 10^4$.

Preparation of Baccatin III Lactate, 3-Phenyllactate, and *N*-Benzoylisoserine Esters 3-8. To a solution of 50 mg (0.066 mmol) of 14, 85 mg (0.39 mmol) of dipyrilidyl carbonate, and 16 mg (0.13 mmol) of 4-(dimethylamino)pyridine in 2.28 mL of toluene at room temperature was added dropwise a solution of 0.39 mmol of 9, 10, or 13 in 1 mL of toluene. The mixture was heated to 70 °C and stirred for 48 h, in the case of 9 and 10, or 6 h in the case of 13, by which time 14 had been consumed. The mixture was cooled, diluted with methylene chloride, washed with aqueous 0.5 N hydrochloric acid, water, and dried (sodium sulfate). Removal of solvent gave material to which was added 64 mg (0.983 mmol) of zinc and 1.3 mL of an acetic acid-methanol mixture (1:1). This reaction mixture was heated to 40 °C for 5 h. After being cooled to room temperature, it was diluted with methylene chloride, filtered to remove zinc salts, washed with aqueous saturated sodium bicarbonate, and dried (sodium sulfate), and the solvent was removed. Purification of the residue by flash chromatography provided, after solvent removal, material that was pure spectroscopically and by TLC analysis. HPLC (Waters instrument; methanol-water, 65:35, in the case of 3-6, or methanol-water-acetonitrile, 20:40:40, in the case of 7 and 8) provided samples for characterization and biological evaluation.

Baccatin III 13-((*R*)-lactate) (3): 53% yield; UV λ_{\max} nm (ϵ) 230 (1.5×10^4); HRFABMS (sodium lauryl sulfate surfactant) calcd 681.2523 (M + Na), obsd 681.2577.

Baccatin III 13-((*S*)-lactate) (4): 51% yield; UV λ_{\max} nm (ϵ) 230 (1.7×10^4); HRFABMS (sodium lauryl sulfate surfactant) calcd 681.2523 (M + Na), obsd 681.2564.

Baccatin III 13-((*R*)-3-phenyllactate) (5): 37% yield; UV λ_{\max} nm (ϵ) 230 (1.9×10^4); HRFABMS (sodium lauryl sulfate surfactant) calcd 757.2836 (M + Na), obsd 757.2874.

Baccatin III 13-((*S*)-3-phenyllactate) (6): 29% yield; UV λ_{\max} nm (ϵ) 230 (2.0×10^4); HRFABMS (sodium lauryl sulfate surfactant) calcd 757.2836 (M + Na), obsd 757.2895.

Baccatin III 13-((*R*)-*N*-benzoylisoserinate) (7): 46% yield; ¹³C NMR δ 203.65, 172.70, 171.19, 170.60, 168.58, 167.02, 142.09, 133.51, 133.19, 129.14, 81.06, 79.08, 58.62, 43.18 (quaternaries), 133.76, 132.03, 130.12, 128.72, 127.03 (double or quadruple signals), 84.41, 75.61, 74.96, 72.15, 71.64, 70.73, 45.74 (CH), 76.48, 43.56, 35.63 (double signal) (CH₂), 26.82, 22.52, 21.71, 20.83, 14.92, 9.56 (CH₃); UV λ_{\max} nm (ϵ) 230 (3.1×10^4); HRFABMS calcd 778.3075 (M + H), obsd 778.3099.

Baccatin III 13-((*S*)-*N*-benzoylisoserinate) (8): 94% yield; ¹³C NMR δ 203.64, 172.73, 171.16, 170.01, 168.41, 167.02, 141.96, 133.79, 133.70, 129.12, 81.04, 79.24, 58.66, 43.13 (quaternaries), 133.15, 131.98, 130.05, 128.71, 127.03 (double or quadruple signals), 84.47, 75.56, 74.94, 72.20, 72.08, 70.17, 45.72 (CH), 77.20, 43.53, 35.90, 35.63 (CH₂), 26.79, 22.42, 21.60, 20.82, 15.25, 9.51 (CH₃); UV λ_{\max} nm (ϵ) 230 (3.1×10^4); HRFABMS calcd 778.3075 (M + H), obsd 778.3123.

Preparation of Microtubules. Calf brain microtubule protein (MTP), which includes ~15-20% microtubule associated proteins, was purified by two cycles of temperature-dependent assembly-disassembly by a procedure modified from Shelanski et al.³¹ and described in detail by Ringel and Horwitz.³² The final buffer solution used for all of the drug-protein studies (MES buffer) contained 0.1 M 2-morpholinoethanesulfonic acid (MES), 1 mM ethyleneglycol bis(β -aminoethyl ether)-*N,N,N',N'*-tetraacetic acid (EGTA), 0.5 mM MgCl₂, and 3 M glycerol at pH 6.6. Samples for electron microscopy were placed on carbon-over-Parlodion-coated grids (300 mesh) and negatively stained with 2% uranyl acetate.

Microtubule Assembly. Microtubule assembly in the presence or absence of drugs was monitored spectrophotometrically by using a spectrophotometer equipped with a thermostatically regulated liquid circulator. The temperature was held at 35 °C and changes in turbidity (representative of polymer mass) were monitored at 350 nm.

(30) Della Casa de Marcano, D. P.; Halsall, T. G. *J. Chem. Soc., Chem. Commun.* 1975, 365.

(31) Shelanski, M. L.; Gaskin, F.; Cantor, C. R. *Proc. Natl. Acad. Sci. U.S.A.* 1973, 70, 765.

(32) Ringel, I.; Horwitz, S. B. *J. Pharm. Exp. Ther.* 1987, 242, 692.

Cell Culture and Immunofluorescence Studies. Murine macrophage-like cell line, J774.2, and Chinese hamster ovary (CHO) cells were maintained as described.³¹ Immunofluorescence studies were performed on CHO cells using a mouse monoclonal antibody against tubulin as the first antibody and a rhodamine-conjugated rabbit anti-mouse antibody as the second antibody.³²

Modelling Calculations. Calculations were performed with MM2 (87) available from the Quantum Chemistry Program Exchange, Department of Chemistry, Indiana University, Bloomington, IN. The following parameters were employed: dielectric constant, 4.0; torsional constants for the 6-1-3-6 atom type angle, $V_1 = 0.0$, $V_2 = -0.6$, $V_3 = 0.3$; torsional constants for the 2-3-9-28 atom type angle, $V_1 = 0.0$, $V_2 = 5.0$, $V_3 = 0.0$.

Acknowledgment. Support through USPHS Grant No. CA 41349 (to C.S.S.) and CA 39821 (to S.B.H.) awarded by the National Cancer Institute, DHHS, and by the Israel Cancer Association (to I.R.) is gratefully acknowledged. The acquisition of major instrumentation at Bryn Mawr was made possible by grants from the Camille

and Henry Dreyfus Foundation, the PQ Corp., the W. M. Keck Foundation, and Merck & Co., Inc.

Registry No. 3, 131760-44-6; 4, 131896-65-6; 5, 131760-45-7; 6, 131896-66-7; 7, 131760-46-8; 8, 131896-67-8; (R)-9, 131760-47-9; (S)-9, 131760-62-8; (R)-9 methyl ester alcohol, 17392-83-5; (S)-9 methyl ester alcohol, 27871-49-4; (R)-9 methyl ester, 131760-51-5; (S)-9 methyl ester, 131760-52-6; (R)-10, 131760-48-0; (S)-10, 131760-63-9; (R)-10 methyl ester alcohol, 27000-00-6; (S)-10 methyl ester alcohol, 13673-95-5; (R)-10 methyl ester, 131760-53-7; (S)-10 methyl ester, 131760-54-8; (R)-11, 57044-25-4; (S)-11, 60456-23-7; (R)-11 *p*-methoxyphenyl ether, 71031-04-4; (S)-11 *p*-methoxyphenyl ether, 71048-65-2; (R)-12, 131760-49-1; (S)-12, 131760-64-0; (R)-12 azide, 131760-56-0; (S)-12 azide, 131760-55-9; (R)-12 azido benzoate, 131760-58-2; (S)-12 azido benzoate, 131760-57-1; (R)-12 trichloroethoxymethyl ether, 131760-59-3; (S)-12 trichloroethoxymethyl ether, 131760-60-6; (R)-13, 131760-65-1; (S)-13, 131760-50-4; 16, 131760-61-7; *p*-methoxyphenol, 150-76-5.

Supplementary Material Available: Preparation and characterization data for 9, 10, 13, and 16 (4 pages). Ordering information is given on any current masthead page.

Positional Effects of Sulfation in Hirudin and Hirudin PA Related Anticoagulant Peptides[†]

Marguerite H. Payne, John L. Krstenansky,* Mark T. Yates, and Simon J. T. Mao

Merrell Dow Research Institute, 2110 East Galbraith Road, Cincinnati, Ohio 45215. Received July 30, 1990

C-Terminal fragment analogues of the leech protein hirudin or the related protein hirudin PA block thrombin's cleavage of fibrinogen. Three series of synthetic peptides were synthesized to study the effects of sulfation in hirudin-derived peptides. Potency of hirudin analogues increased with *p*-(amino)Phe⁶³, *p*-(aminosulfonate)Phe⁶³, and *p*-(sulfate)Tyr⁶³ substitution in place of Tyr⁶³. Sulfation of Tyr⁶³, which in hirudin is normally Phe, resulted in a loss of 1 order of magnitude in potency. The sulfation of Tyr⁶⁴ of the hirudin PA related analogue resulted in increased potency as for the hirudin analogue. However, in this series the *p*-(amino)Phe⁶⁴ and *p*-(aminosulfonate)Phe⁶⁴ did not have increased potency. In addition to these positional effects, replacing all the Glu residues with (O-sulfato)Ser yielded an analogue with full antithrombin potency.

Introduction

Peptide derivatives of hirudin's C-terminal functional domain are antithrombin agents that bind thrombin at a noncatalytic site, preventing its procoagulant actions.¹ While the lipophilic residues of the hirudin peptides are essential to potent interaction with thrombin,² these peptides are anionic and some of their charged residues are involved in direct interactions with thrombin.³ In particular, the X-ray crystallographic structure of the hirudin-thrombin complex shows that Asp⁵⁵ and Glu⁵⁷ of hirudin are involved in interactions with basic residues on the surface of thrombin.³ Additionally, sulfation of Tyr⁶³ may add some ionic interactions to the overall binding energy of hirudin.^{3,4} Hirudin is a member of a family of anticoagulant proteins isolated from bloodsucking leeches. Most known variants of this family of proteins share the hirudin C-terminal amino acid sequence. The only known exceptions are hirudin PA⁵ and hirullin P18,⁶ which have significant differences in their sequences in this region.

Hirullin P18 does not contain a Tyr residue near its C-terminus that could be sulfated as in hirudin although it shares the same functional role in the protein.⁷ Hirudin PA contains a sulfated Tyr residue in its C-terminal functional domain, but its location is shifted by one position relative to hirudin. Structure-activity relationships of the unsulfated hirudin and hirudin PA C-terminal peptide analogues are comparable.^{8,9} However, a comparison of sulfated and nonsulfated hirudin PA analogues or sulfated hirudin and sulfated hirudin PA analogues has not been reported.

Sulfate groups are known to be capable of strong interaction with basic residues of proteins. Heparin can bind tightly to specific regions of proteins using almost exclu-

* Present address: Syntex Research, 3401 Hillview Avenue, Palo Alto, California 94303.

[†] All amino acids are the L enantiomer unless otherwise noted. Abbreviations used include: Boc, *tert*-butyloxycarbonyl; 2-BrZ, 2-bromobenzoyloxycarbonyl; Bzl, benzyl; Cha, β -cyclohexylalanine; DCC, *N,N'*-dicyclohexylcarbodiimide; DCM, dichloromethane; DMF, dimethylformamide; HOBT, *N*-hydroxybenzotriazole; Pnh, *p*-aminophenylalanine; Pno, *p*-nitrophenylalanine; SO₂, pyridine, sulfur trioxide pyridine complex; Suc, succinyl; TFA, trifluoroacetic acid.

- (1) Krstenansky, J. L.; Mao, S. J. T. *FEBS Lett.* 1987, 211, 10.
- (2) Krstenansky, J. K.; Owen, T. O.; Yates, M. T.; Mao, S. J. T. *J. Med. Chem.* 1987, 30, 1688.
- (3) Rydel, T. J.; Ravichandran, K. G.; Tulinsky, A.; Wolfram, B.; Huber, R.; Roitsch, C.; Fenton, J. W. *Science* 1990, 249, 277.
- (4) Stone, S. R.; Dennis, S.; Hofsteenge, J. *Biochemistry* 1989, 28, 6857.
- (5) Dodt, J.; Machleidt, W.; Seemuller, U.; Maschler, R.; Fritz, H. *Biol. Chem. Hoppe-Seyler* 1986, 367, 803.
- (6) Maschler, R.; Steiner, V.; Grutter, M. G.; Fritz, R. Eur. Patent Applic. 1989, EP-A-0347376.
- (7) Krstenansky, J. L.; Owen, T. J.; Yates, M. T.; Mao, S. J. T. *FEBS Lett.* 1990, 269, 425.
- (8) Krstenansky, J. K.; Owen, T. J.; Yates, M. T.; Mao, S. J. T. *Thromb. Res.* 1988, 52, 137.
- (9) Krstenansky, J. L.; Broersma, R. J.; Owen, T. J.; Payne, M. H.; Yates, M. T.; Mao, S. J. T. *Thromb. Haemostasis* 1990, 63, 208.